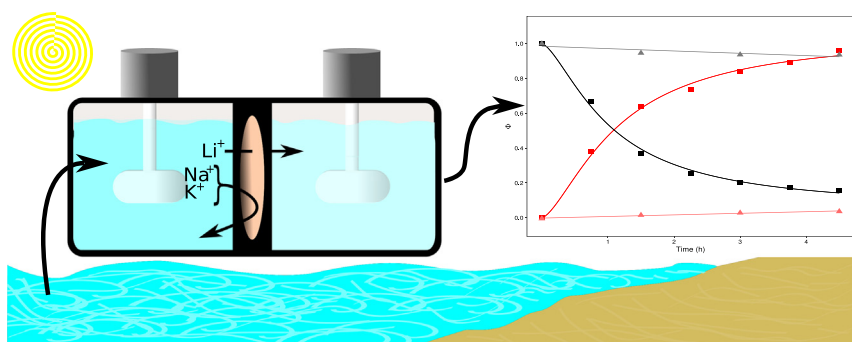


Selective lithium extraction and concentration from diluted alkaline aqueous media by a polymer inclusion membrane and application to seawater

Cristhian Paredes, Eduardo Rodríguez de San Miguel*

Departamento de Química Analítica, Facultad de Química, UNAM, Ciudad Universitaria, 04510 Ciudad de México, Mexico

GRAPHICAL ABSTRACT



ARTICLE INFO

Keywords:

Lithium recovery
Polymer inclusion membranes
Synergistic extraction
Seawater
Valuable metals

ABSTRACT

A method capable of selectively extracting and concentrating lithium from diluted alkaline aqueous media is proposed using a polymer inclusion membrane composed of cellulose triacetate (CTA) and the carriers LIX-54-100 and Cyanex 923 without the addition of plasticizer. Transport conditions were optimized using the modified simplex algorithm. The system can transport lithium against its concentration gradient due to a coupled hydrogen ions countertransport. Under optimized conditions, the membrane can be reused up to 10 times before losing 40% of its initial capacity. Using the proposed system, lithium can be concentrated from diluted aqueous media in presence of high quantities of other metallic cations to get a lithium chloride solution from which it would be easier to get valuable high purity lithium compounds. The membrane was used to extract and concentrate lithium from synthetic and natural seawater and good selectivity and recovery were achieved.

1. Introduction

Lithium has become a strategic element since modern lifestyle requires us to have efficient and lightweight ways to store energy [1,2].

As the lightest solid element having also the higher redox potential and heat capacity, lithium fits perfectly many of our necessities due to its excellent energy storage density besides many other useful properties of its compounds. Lithium natural reserves exist mainly in hard rock and

Abbreviations: PIM, polymer inclusion membrane; CTA, cellulose triacetate; PVC, poly(vinylchloride); FAES, Flame Atomic Emission Spectrometry; FAAS, Flame Atomic Absorption Spectrometry; RPM, revolutions per minute; FPS, frames per second; RGB, red green blue

* Corresponding author.

E-mail address: erdsmsg@unam.mx (E. Rodríguez de San Miguel).

<https://doi.org/10.1016/j.desal.2020.114500>

Received 7 February 2020; Received in revised form 28 April 2020; Accepted 29 April 2020

0011-9164/ © 2020 Elsevier B.V. All rights reserved.

clay minerals and brines of salt lakes, geothermal water, groundwater, and seawater. The extraction process from solids involves high cost-demanding and environment-hazardous operations and an increasingly scarce raw material. On the other hand, extracting the lithium that is present in natural liquid sources is usually accomplished by cheaper hydrometallurgy processes which have the advantage of having the element already present in solution. The fast-growing demand for this element could overcome the predicted availability by the next few decades [3,4]. The growing lithium demand is greatly influenced by a transport sector shifting to electric propulsion as a low-carbon technology in a world looking for stop climate change [5]. In these terms, more research is required to find practical ways to extract lithium from resources that are not currently being extracted due to economic constraints that mainly arises from a very low lithium concentration and a high relative concentration of other species.

Oceans compose the biggest known earth's lithium reserves. The water in the oceans has an estimated total volume of $1.37 \times 10^9 \text{ km}^3$ and an average lithium concentration of $0.17\text{--}0.18 \text{ mg kg}^{-1}$ [2,6,7]. Total lithium amount in the oceans (250 million tons) is much bigger than the combined resources of the lithium-rich countries (14 million tons) [8]. Lithium extraction from seawater is not currently possible at the industrial scale for the reasons mentioned above [3].

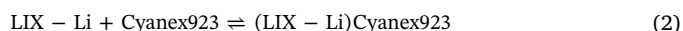
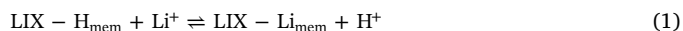
The predicted shortages of the element may cause inflation in the cost making economically viable its extraction from very diluted media. Several strategies like solvent Extraction (SX) [9–11], combined cation exchange membranes [12,13], specific adsorption [14], selective electrolysis and electrodialysis [7,8,15], nanofiltration [16,17], supported liquid membranes (SLM) [18–21] and recently, polymer inclusion membranes (PIM) [22] has been studied to extract lithium from liquid sources. Some of these methods have not been applied to real sample matrices and most of them are far from being implemented at industrial scale.

Carrier mediated lithium extraction using SX and SLMs usually involves the use of two carriers that present synergism when used together. The mixture of acidic bidentate carriers with neutral solvating carriers saturates the lithium 4-sites coordination sphere creating a lipophilic neutral compound [23]. Harvianto et al. reported the use of TTA (thenoyltrifluoroacetone) and TOPO (trioctylphosphine oxide) in kerosene to extract lithium from seawater and achieved 65% efficiency [24]. The same extractants were later used by Cai et al. in the first report of a PIM for the extraction of lithium from synthetic solutions [22]. The synergistic solvent extraction of lithium ions from chloride solutions using LIX-54-100 and Cyanex 923 carriers was firstly reported by Pranolo et al. [9] and the authors achieved a 97% lithium recovery in a synthetic solution containing the monovalent ion sodium and obtained good selectivity. Similar approaches have been widely applied to several SLM lithium extractions [11].

A polymer inclusion membrane (PIM) is a non-porous physical barrier that incorporates extractants (carriers) and a plasticizer into a polymer matrix usually made of cellulose triacetate (CTA) or poly(vinyl chloride) (PVC) [25]. Similar in operation and performance to supported liquid membranes (SLM) which is a porous physical barrier that holds an organic solution of the extractants inside the channels of the membrane [26], PIMs have demonstrated good suitability to extract several valuable metals from seawater overcoming the stability issues commonly related to the use of some SLM systems [27].

Here we present a PIM system capable of selectively extracting and concentrating lithium ions from seawater after two not highly energy-demanding precipitation steps. The synergistic solvent extraction of lithium ions from chloride solutions using LIX-54-100 and Cyanex 923 carriers was firstly reported by Pranolo et al. [9]. Similar approaches have been applied to several SLM lithium extractions [11]. SLM and PIM systems present the advantage over traditional solvent extractions that they use smaller carriers amounts and allow the extraction and stripping steps to be performed simultaneously in processes that can be adapted to work on continuous flow settings [25].

LIX-54-100 (main component 1-phenyldecanone-1,3-dione [28]) is a β -diketone chelating carrier that presents keto-enol tautomerism. In the enolic form, it is capable of reversely exchange the mildly acidic proton by a lithium cation producing a neutral chelate than can be solvated and transported across the membrane by the Cyanex 923 (main component trialkylphosphine oxide, with hexyl and octyl groups [29]). Several β -diketones and solvation extractants have been combined to synergistically extract lithium ions using membranes [11,22]. Involved reactions are lithium chelation by LIX-54-100 before neutral chelate solvation by Cyanex 923:



The above reactions occur as written in the feed side of the membrane-solution interface and occur in the reverse direction at the strip side of the membrane-solution interface. The driving force is a marked hydronium concentration gradient between the acidic strip solution and the alkaline feed solution. Transport of metal cations can proceed until this proton gradient vanishes but the process may be limited by membrane stability.

In this work lithium recovery and concentration using a PIM system containing the synergic LIX-54-100/Cyanex 923 extractant mixture is optimized and studied in terms of its efficiency factors (permeability, selectivity and stability) with the aim of evaluating its potentiality as a separation method of the metal from diluted alkaline aqueous media. An application to synthetic and natural seawaters is presented as well.

2. Experimental

2.1. Reagents and apparatus

All aqueous solutions were prepared using analytical grade reagents and deionized water. Extractants Cyanex 923 and LIX-54-100 were kindly provided by Cytec Canada Inc. and Cognis Corporation, respectively. Cellulose triacetate (CTA, Aldrich. Acetyl content 43.6 wt%, M_w 72,000 to 74,000 g mol^{-1}), dichloromethane (DCM, J.T. Baker), sodium chloride (Monterey), potassium chloride (Merck), calcium chloride dihydrate (Merck), magnesium sulfate heptahydrate (Merck), hydrochloric acid (Sigma-Aldrich), ammonia hydroxide (Sigma-Aldrich), diammonium hydrogen phosphate (Merk) and sodium hydroxide (Mallinckrodt) were used. Lithium and magnesium chloride solutions were prepared by dissolving the respective carbonates (Aldrich) in stoichiometric diluted hydrochloric acid. All reagents were used without further purification.

Lithium, sodium and potassium ions concentrations were determined by Flame Atomic Emission Spectrometry (FAES, Perkin–Elmer 3100 atomic absorption spectrometer). Calcium and magnesium ion concentration were determined by Flame Atomic Absorption Spectrometry (FAAS, Perkin–Elmer 3100 atomic absorption spectrometer). The analysis were performed under manufacturer recommended conditions. Most determinations were made using external standard calibration with matrix matching. Lithium determination on the seawater matrix was made using a single-point standard addition method [30].

2.2. Polymeric inclusion membranes preparation

Membranes were prepared by the casting-evaporation procedure described elsewhere [31]. Weighed amounts of the base polymer and extractants were dissolved in 10 mL DCM by magnetic stirring for at least 2 h. The homogeneous solution was quantitatively transferred to a 5 cm diameter Pyrex® glass Petri dish, loosely covered and allowed to slowly evaporate overnight. Transparent homogeneous films were formed. Flooding the Petri dish with water facilitated the membrane peeling off from the glass.

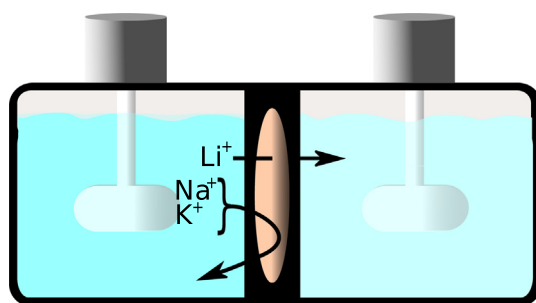


Fig. 1. Scheme of permeation cell used.

Table 1

Cations present in the simplified synthetic seawater recipe used.

Cation	Conc. (mg kg ⁻¹)	Relative molar ratio
Na ⁺	10,780	18,000
Mg ²⁺	1280	2030
Ca ²⁺	415	400
K ⁺	390	390
Li ⁺	0.18	1

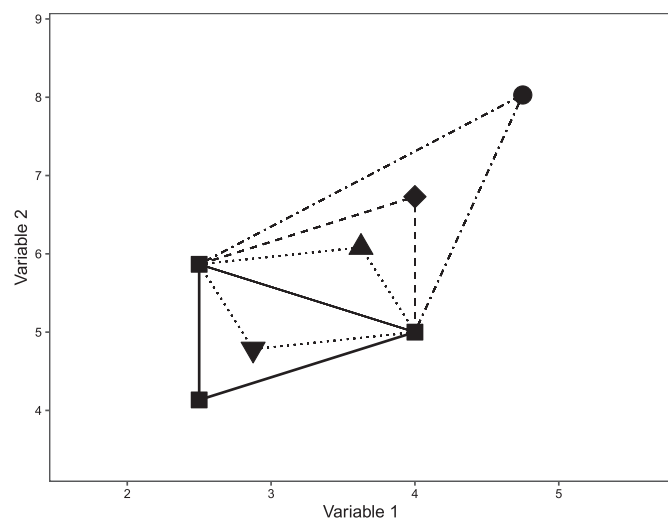


Fig. 2. Possible movements in a two-dimensional simplex. Original vertices (squares), reflection (square rotated 45°), expansion (circle), contraction on the reflection side (up-pointing triangle) and contraction on the worst vertex side (down-pointing triangle).

Table 2

Starting simplex coordinates.

	X1	X2	X3	X4	β^{-1}
Start	70	2.00	0.010	0.07	–
Step size	20	1.00	0.010	–0.06	–
Vertex 1	70.0	2.00	0.010	0.07	0.487
Vertex 2	50.0	2.75	0.010	0.07	0.397
Vertex 3	50.0	1.75	0.016	0.07	0.254
Vertex 4	50.0	1.75	0.007	0.04	0.268
Vertex 5	50.0	2.75	0.007	0.04	0.345

Membranes were flexible and had good mechanical strength despite the absence of plasticizer in its formulation. As reported in several studies [22,32,33], this is possible due to the double function carrier/plasticizer by one of the extractants. We found that the transport process had better repeatability when the membrane side that was against the glass surface (smoother than the air-exposed side) was facing the source solution. Membrane thickness was measured using a Fowler

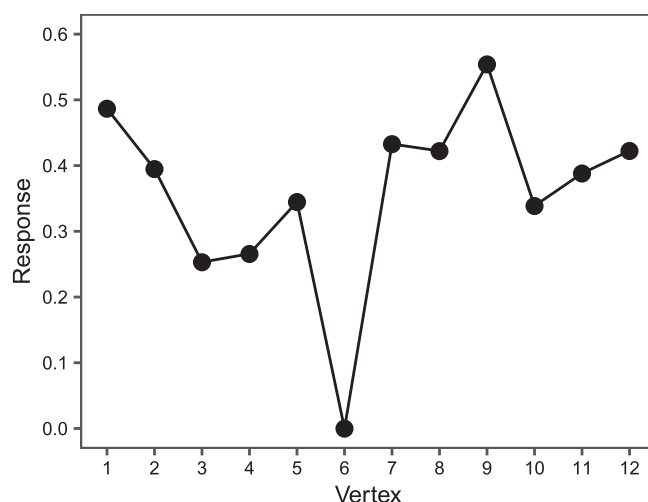
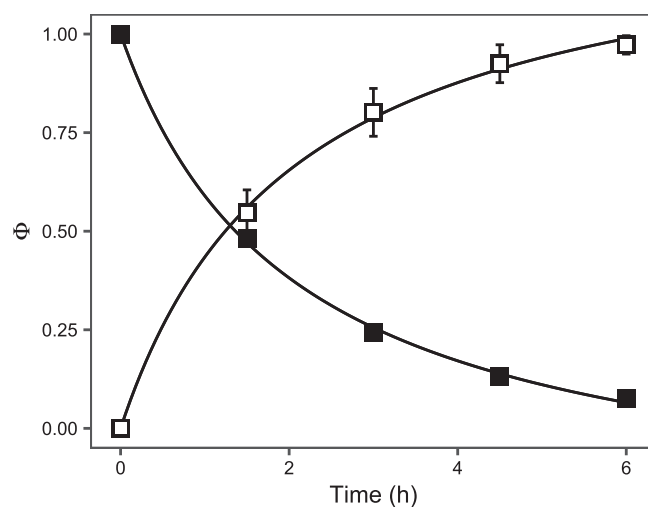


Fig. 3. Response against vertex number in simplex optimization. Best results at vertex 9.

Table 3

New vertices evaluated during optimization. Movements R, Cw and E means reflection, contraction on the worst vertex side and expansion of the simplex, respectively. For details see reference [46].

Vertex	Movement	X1	X2	X3	X4	β^{-1}
6	R	60.0	2.88	0.000	0.04	0.000
7	Cw	52.5	2.03	0.012	0.06	0.434
8	R	61.2	3.02	0.013	0.08	0.424
9	R	66.8	2.15	0.016	0.10	0.554
10	E	75.3	1.85	0.020	0.13	0.343
11	R	75.3	1.85	0.016	0.09	0.388
12	Cw	56.3	2.52	0.011	0.07	0.422

Fig. 4. Lithium transport profile for feed (filled squares) and strip (void squares) solutions under optimized conditions. Feed solution: NH₄OH 0.016 mol kg⁻¹ and LiCl 2 mg kg⁻¹ as Li⁺. Strip solution: HCl 0.10 mol kg⁻¹.

IP54 digital gauge screw micrometer.

2.3. Transport experiments

A 200 mL permeation cell (Fig. 1) was used. The membrane exposed area was 19.6 cm² and the initial amount of solution at each side of the cell was 85 mL. After system optimization, the strip solution was 0.10 mol kg⁻¹ hydrochloric acid while the feed solution was composed of

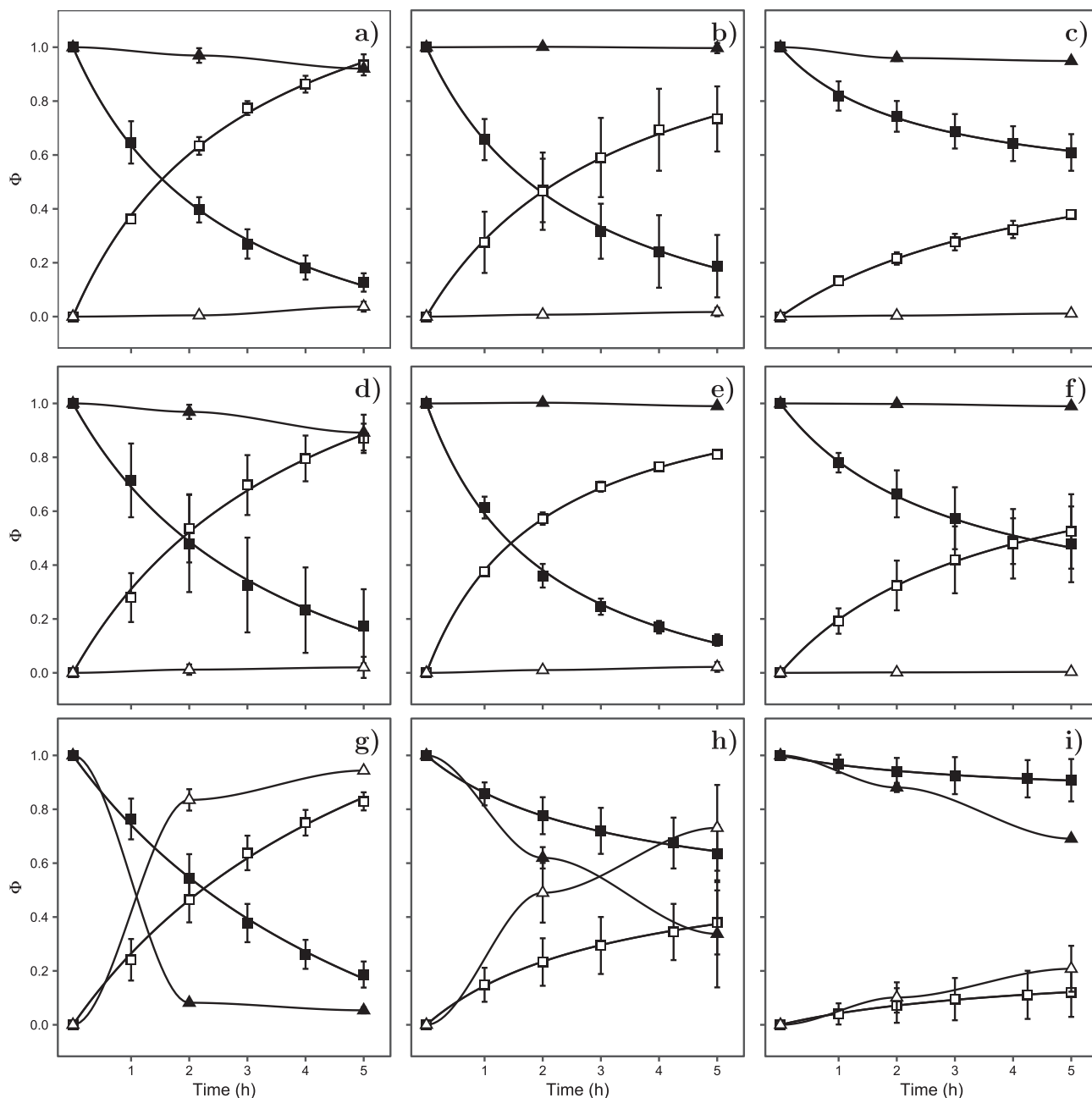


Fig. 5. Transport profiles for the systems containing lithium (squares) and other cation (triangles): Na^+ 1:1 (a), Na^+ 1:10 (b), Na^+ 1:100 (c), K^+ 1:1 (d), K^+ 1:10 (e), K^+ 1:100 (f), Mg^{2+} 1:1 (g), Mg^{2+} 1:10 (h) and Mg^{2+} 1:100 (i). Feed fractions are in filled polygons and strip fractions are in void polygons. Feed solution: NH_4OH $0.016 \text{ mol kg}^{-1}$, LiCl 2 mg kg^{-1} as Li^+ and secondary cation (Na^+ , K^+ or Mg^{2+}) chloride salt in respective molar ratio. Strip solution: HCl 0.10 mol kg^{-1} .

Table 4
Separation factors between lithium and other cations at several mole ratios.

Cation	Mole ratio		
	1:1	1:10	1:100
Na^+	5.4	47	33
K^+	8.0	36	122
Mg^{2+}	0.87	0.55	0.60

$0.016 \text{ mol kg}^{-1}$ ammonium hydroxide. Lithium initial concentration in feed phase was kept constant at 2 mg kg^{-1} . Solutions were mechanically stirred at $600 \pm 50 \text{ RPM}$. The agitation speed was determined using a high-speed camera (240 FPS) and the RGB profile tool of the Open Source Physics video processing software Tracker [34]. Under

these hydrodynamic conditions, we found little to no dependency on the agitation speed on transport efficiency. Small aliquots were taken at regular time intervals to monitor metal concentration changes in the solutions.

For the selectivity studies, feed solutions were added with Na^+ , K^+ and Mg^{2+} at molar ratios $\text{M}^{n+}/\text{Li}^+$ 1:1, 10:1 and 100:1. Corresponding mass ratios were as high as 331:1, 563:1 and 350:1 for Na^+ , K^+ and Mg^{2+} , respectively.

Membrane reuse capabilities were tested by changing feed and strip solutions 10 times each 6 h. The strip compartment was soaked with deionized water between cycles. Concentration experiments were made renewing feed solution 5 times every 6 h while using the same membrane and strip solution.

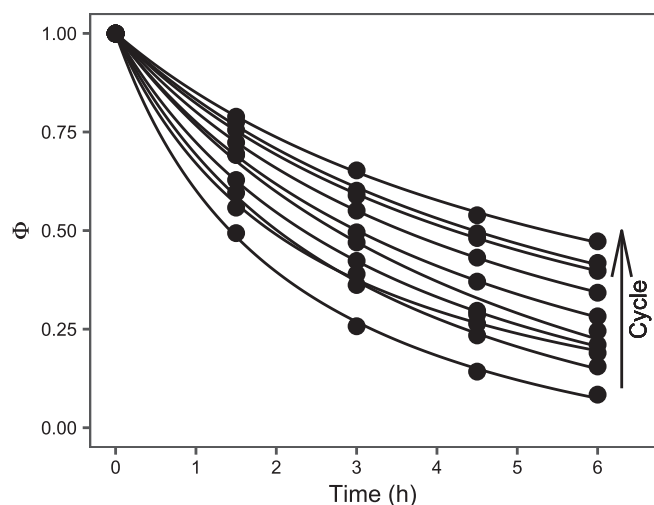


Fig. 6. Lithium depletion profiles from feed solution for several cycles using the same membrane. Feed solutions: NH_4OH $0.016 \text{ mol kg}^{-1}$ and LiCl 2 mg kg^{-1} as Li^+ . Strip solutions: HCl 0.10 mol kg^{-1} .

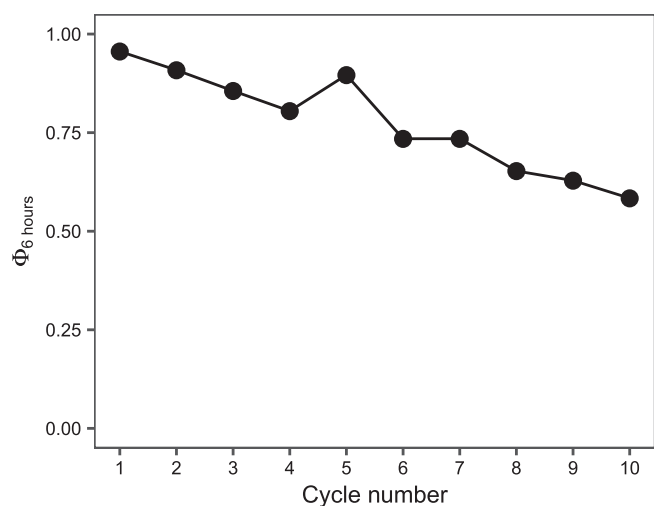


Fig. 7. Lithium transported fraction to the strip phase after 6 h reusing the same membrane several times. Feed solutions: NH_4OH $0.016 \text{ mol kg}^{-1}$ and LiCl 2 mg kg^{-1} as Li^+ . Strip solutions: HCl 0.10 mol kg^{-1} .

2.4. Artificial and natural seawater experiments

The artificial seawater matrix was made according to the simplified synthetic seawater recipe used to determine thermodynamic properties on seawater [35]. In this recipe, natural occurring concentrations of bromide and fluoride ions are replaced by chloride while strontium is replaced with calcium. Most species having lower concentrations are not considered. The ionic strength of this solution is the same as that of natural seawater [36]. As lithium has a very low concentration in seawater, is not reported in the recipe and then was added to the solution at the average reported concentration of 0.18 mg kg^{-1} ($2.6 \times 10^{-5} \text{ mol kg}^{-1}$) [2]. Cations concentrations used are listed in Table 1. Sulfate and chloride concentrations were 0.028 and 0.55 mol kg^{-1} , respectively.

Natural seawater samples were hand-collected along two shores in the Gulf of México and the Caribbean Sea. The samples were filtered to remove large solids and remained refrigerated until use. Both samples were mixed since no big differences were found regarding pH and lithium, sodium, potassium, calcium and magnesium concentration. The concentration of those cations in the natural samples was very close to

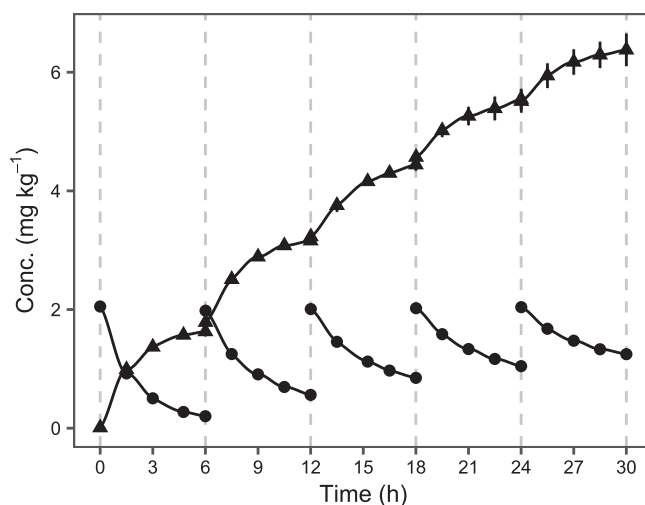


Fig. 8. Lithium concentration profile for feed (circles) and strip (triangles) solutions in concentration study. Dashed vertical lines indicate the renewal of feed solutions. Feed solution: NH_4OH $0.016 \text{ mol kg}^{-1}$ and LiCl 2 mg kg^{-1} as Li^+ . Strip solution: HCl 0.10 mol kg^{-1} .

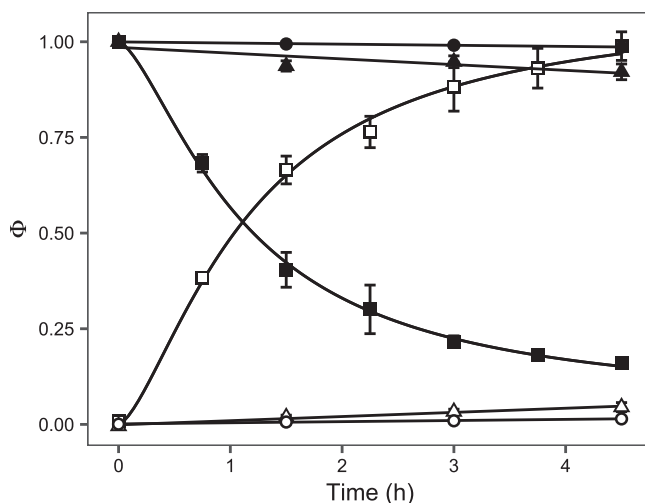


Fig. 9. Transport profiles for lithium (squares), sodium (triangles) and potassium (circles) in synthetic seawater extraction experiments. Feed fractions are in filled polygons and strip fractions are in void polygons. Feed solution: synthetic seawater (Table 1) with free OH^- concentration of 0.02 mol kg^{-1} . Strip solution: HCl 0.10 mol kg^{-1} .

that in the artificial seawater (Table 1).

Transport studies involving both synthetic and natural seawater were performed after magnesium and calcium were almost completely removed by stepwise precipitation/centrifugation using initially sodium hydroxide at a final concentration of 0.15 mol kg^{-1} and then diammonium hydrogen phosphate at a final concentration of $0.005 \text{ mol kg}^{-1}$. The solution was used without ammonium hydroxide addition as long as excess hydroxide ions that did not precipitate in the first magnesium and calcium removal provided a media alkaline enough to allow lithium transport.

Lithium concentration process from natural seawater was made in the same way that the concentration experiments described above but the cycle time shortened to 4.5 h.

2.5. Data treatment and transport optimization

Data analysis and visualization were made in open-source statistical software R [37] mainly using the CRAN R-package `transmem` designed

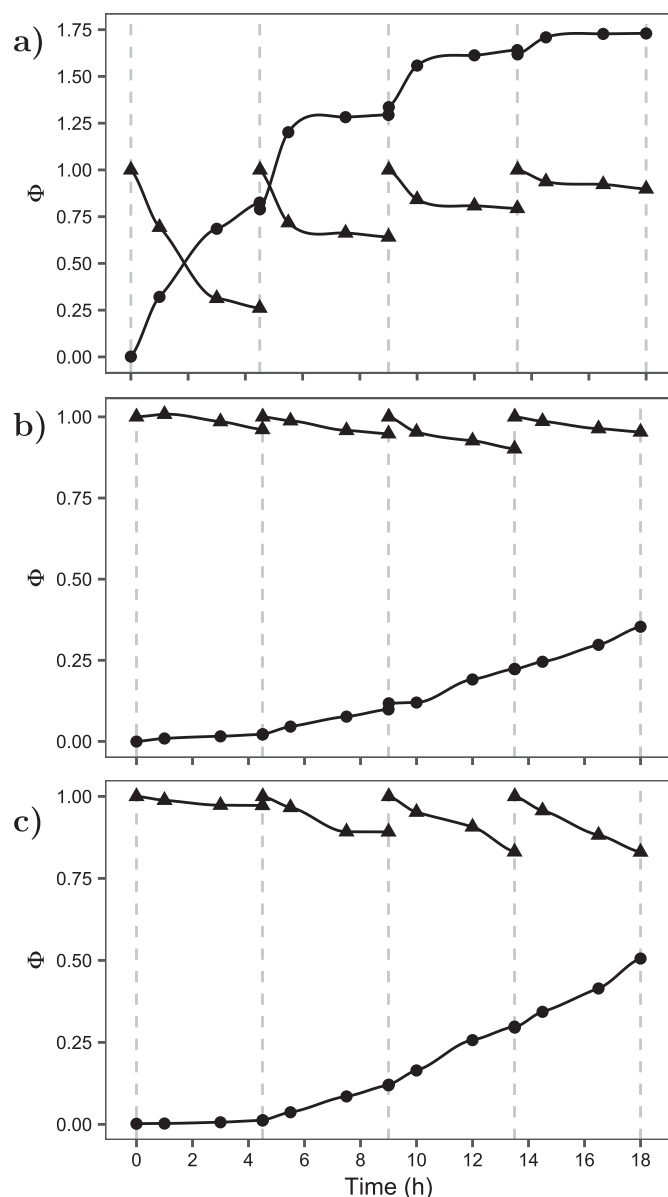


Fig. 10. Transport profiles in feed (triangles) and strip (circles) solutions for lithium (a), sodium (b) and potassium (c) in lithium extraction and concentration experiments using natural seawater. Dashed vertical lines indicate the renewal of feed solution. Feed solution: synthetic seawater (Table 1) plus free $[\text{OH}^-]$ concentration of 0.02 mol kg^{-1} . Strip solution: $\text{HCl } 0.10 \text{ mol kg}^{-1}$.

to organize and represent data of membrane transport processes [38].

To help in the comparison of the experiments, the transport profiles of lithium were adjusted to Eqs. (3) and (4) for the strip and feed phases, respectively.

$$\Phi_{Lis} = \frac{\alpha_s t^\gamma}{\beta_s + t^\gamma} \quad (3)$$

$$\Phi_{Lif} = 1 - \frac{\alpha_f t^\gamma}{\beta_f + t^\gamma} \quad (4)$$

where t is time in hours, α is an adjustable parameter related to the maximal transported fraction and β is another adjustable parameter that relates the time at which the transported fraction is a given fraction (e.g. the half) its maximal value. The subscripts s and f relates to the strip or the feed phase, respectively. The model resembles the Michaelis-Menten enzymatic kinetic model [39] with the inclusion of a

parameter γ which is used only to enhance fitness and does not need to be changed to compare systems under similar conditions (e.g. along an optimization). If γ is equal to 1 (as in most cases), then β is the time at which the transported fraction is half its maximal value.

The values α and β and their associated uncertainties can be found by non-linear regression using the Gauss-Newton algorithm [40] but the value of γ must be decided according to the eccentricity of the data under study. The transport process is said to be more efficient for higher values of α and lower values of β . If no metal is accumulated in the membrane, the parameters are expected to be the same for both phases. This allows their respective unification by weighted averaging considering each estimate quality (i.e. associated error due to lack of fitness). The parameters can be used (individually or combined by a desirability function) to optimize the system using design of experiments. A similar approach was previously reported by our group using factorial and central composite experimental designs to optimize a PIM system for chromium(VI) transport using adjustable parameters of empirical functions that describe the evolution of the system in time [41].

Lithium permeability coefficient as derived by integrated Fick's law can be obtained by the slope of the linear regression considering lithium concentrations changes in time in the feed solution, the solution's volume V and the membrane exposed area a [20].

$$\ln \left(\frac{C_{\text{Li}^+}}{C_{\text{Li}^+}^0} \right) = - \frac{P a}{V} t \quad (5)$$

The separation factor between lithium and other cation is defined as their concentration ratio $\text{Li}^+/\text{M}^{n+}$ in the strip solution at any given time different from zero divided by the initial value of this ratio in the feed solution [42]. Other definitions referring to the ratio in the feed solution at the same given time [21,43] are more adequate for continuous membrane systems and will not be used. The separation factor should equal 1 at the beginning of the experiment indicating that no species has been separated yet. Higher separation factors indicate better selectivity for the interest species and separation factors smaller than 1 indicates that the undesired species is transported preferably across the membrane.

$$S_F(AB) = \frac{C_{\text{Li}^+,s}/C_{\text{M}^{n+},s}}{C_{\text{Li}^+,f}^0/C_{\text{M}^{n+},f}^0} \quad (6)$$

where concentrations may be in mole or mass units, subscripts s and f indicates strip and feed, respectively. The superscript 0 indicates initial value.

The optimization was performed using the simplex algorithm initially proposed by Spendler [44] and later modified by Nelder and Mead [45]. In the simplex optimization algorithm, each experimental variable represents a dimension in an abstract space in which the experiments define points called vertexes. A simplex is a geometric element defined as the simpler polytope possible in a n -dimensional space. The simpler polytope is formed by $n + 1$ vertexes meaning that initial simplex evaluation of n variables will require $n + 1$ experiments. The simplexes in two and three-dimensional spaces are the well-known triangle and tetrahedron, respectively. After performing the experiments and a response has been assigned, one of the vertexes is discarded in favor of a new one that must be evaluated. The discarded vertex is the one with the worst response in the initial simplex or the second worst vertex in the previous simplex. Discarding a vertex and generating a new one is called a simplex movement. Possible movements in a two dimensional simplex are illustrated in Fig. 2. The process can be repeated until the optimum is reached or a response good enough is obtained. The algorithm has proven to be very useful for industrial and laboratory applications [46].

The algorithms were implemented in R and is available as the package `labsimplex` [47]. The optimization objective was to improve the speed of the transport process as long as transport efficiency and selectivity varied slightly with membrane and solution compositions. As

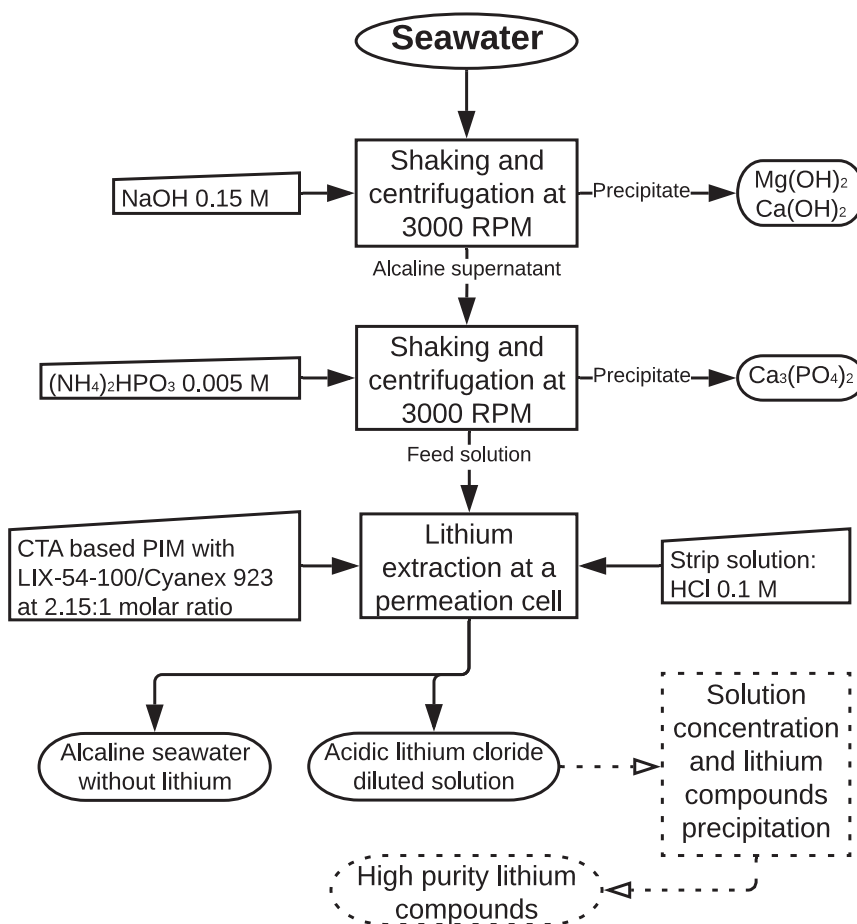


Fig. 11. Flow diagram of the lithium recovery process from seawater. Dashed paths indicate steps that were not considered in the present work.

mentioned above, while higher values of α relates to better final transport efficiency, smaller values of β represented faster transports. For this reason, the simplex optimization consisted on the minimization of the parameter β (or equivalently, the maximization of its inverse).

The separation factor Li^+/Na^+ was monitored in all transports during the optimization process to ensure that the selectivity was not sacrificed while improving lithium flux to the strip solution. For this purpose, sodium chloride was added to the feed solution at a molar ratio $\text{Na}^+:\text{Li}^+$ of 10:1.

3. Results and discussion

3.1. System optimization and uphill lithium transport

A regular initial simplex was constructed using the starting point and step size described in Table 2. The values of the variables (i.e. coordinates) of the experiments (i.e. vertexes) in resulting initial simplex are shown in the same Table. Variables studied were total carriers mass (X1, in mg), molar ratio LIX-54-100/Cyanex 923 (X2) assuming a molar mass of 246 and 348 g mol^{-1} for LIX-54-100 and Cyanex 923, respectively [28,29], ammonium hydroxide concentration in feed solution (X3, in mol kg^{-1}) and hydrochloric acid concentration in strip solution (X4, in mol kg^{-1}). The mass of base polymer was kept constant at 30 mg as it was determined that smaller amounts did not provided enough mechanical resistance to the membrane and higher values decreased lithium permeability.

Evolution in response against vertex number is shown in Fig. 3. Simplex movements are shown in Table 3. The starting point (vertex 1) provided a good response but a better local maxima is found in the ninth experiment.

Optimized membrane composition was 30 mg CTA as base polymer and 67 mg of the carriers in a molar ratio LIX-54-100/Cyanex 923 of 2.15:1. Final membrane mass and average thicknesses were 97 ± 2 mg and 14 ± 4 μm . The optimal carriers molar ratio is close to that previously reported in lithium solvent extraction by Pranolo et al. [9]. Under optimized conditions, lithium ions were completely transported to the strip phase within the first 6 h. No appreciable metal transport was observed when membranes containing only LIX-54-100 or Cyanex 923 were used. The transport profile under optimized conditions is shown in Fig. 4.

Metal accumulation in the membrane polymeric matrix can be determined by mass balance considering lithium fractions in both solutions. If the sum of the two values is significantly lower than 1, then some of the lithium is being retained in the membrane. No lithium significant accumulation is observed as the sum of feed and strip lithium fractions are between 1.00 and 1.05. Under these conditions, the lithium permeability coefficient is $2.1 \times 10^{-5} \text{ m s}^{-1}$, similar to that reported in other liquid membranes systems for lithium transport [19,20,22].

3.2. Selectivity

Transport profiles for systems having lithium and other cations in feed solutions at several molar ratios are shown in Fig. 5. Final separation factors are summarized in Table 4. The system does not significantly transport neither sodium nor potassium. Magnesium is transported to the strip solution more efficiently than lithium does, even when magnesium concentration is two orders of magnitude higher than lithium concentration.

Poor selectivity towards magnesium in most lithium extraction

systems has been attributed to their almost identical ionic ratio [48] being 69 and 72 pm for lithium and magnesium, respectively. Also, magnesium as a divalent cation will be more strongly solvated by the LIX-54-100 than lithium. The system is then expected to exhibit poor selectivity towards the divalent cation calcium too. The application of the proposed system to a real water sample requires precipitation of magnesium and calcium ions from the solution before being fed to the system.

Permeability coefficients for sodium and potassium are low enough to avoid a significative fraction being transported to the strip solution in short times. However, their fluxes (defined as permeability coefficient multiplied by ion concentration on the feed solution [22]) are not insignificant and led to lithium flux diminution when present.

3.3. Membrane reuse and lithium concentration

The membrane had good performance when used several times but transport efficiency gradually decreases after each cycle. Fig. 6 shows the lithium depleted from the feed phase in 10 six-hour cycles. The final transported fraction to the strip phase after each cycle is shown in Fig. 7. Membrane instability arises from the fact that LIX-54-100 is lixiviated from the membrane to the feed solution as long as acid β -diketones solubility in aqueous solution increases with pH [49]. Transport efficiency in the tenth cycle is 61% of that in the first cycle meaning a 40% loss of capacity.

In lithium concentration experiments, only the feed solution was replaced between cycles. The transported fractions are shown in Fig. 8. As mentioned above, lithium transport proceeds against the concentration gradient due to hydronium ions coupled counter-transport. Lithium concentration on strip phase raises to almost three times the initial feed concentration after five six-hour cycles. As seen before, a decrease in the transport efficiency is observed after each feed solution replacement and longer times will be necessary to deplete the same lithium fraction from the feed solutions.

3.4. Synthetic and natural seawater lithium extraction

Magnesium and most calcium ions were precipitated from both artificial and natural seawater as hydroxides by adding sodium hydroxide to a final concentration of 0.15 mol kg^{-1} . Remaining calcium ions were precipitated in a second step by adding diammonium hydrogen phosphate to a final concentration of $0.005 \text{ mol kg}^{-1}$. Each precipitation step involved mechanical shaking of solution for 5 min and centrifugation at 3000 RPM for 5 min. As a consequence of the precipitation process, sodium ion concentration in feed solution increases from 0.47 mol kg^{-1} to 0.62 mol kg^{-1} and very low residual phosphates remain in solution. Excess hydroxide concentration was then enough to keep the desired hydronium concentration gradient that works as a driving force for the lithium transport to the strip solution.

Transport profiles for lithium, sodium and potassium for the synthetic seawater matrix in extraction studies are shown in Fig. 9. There is apparent total lithium transport to the strip solution but in the feed phase at the end of the process, there seems to be a remaining 15% of initial lithium present. This may be attributed to a translational matrix effect in the lithium quantification by FAES. Translational matrix effect can not be compensated by using the standard addition method as long as this method only corrects rotational matrix effects [30].

Considering the data of strip solution, lithium is transported with an efficiency between 96% and 100% within four hours and a half. Only 5% and 1.5% of sodium and potassium ions are transported to the strip solution, respectively. Separation factors of 55 and 120 are reached for sodium and potassium, respectively.

The lithium extraction from natural seawater raised up the pH of the strip solution due to sodium and potassium ions being transported across the membrane with the respective hydrogen ion exchange. If hydronium ions concentration gradient is not high enough, no lithium

transport occurs. To achieve lithium concentration, it was necessary to determine hydronium ions concentration in the strip phase at the end of each cycle and reset its value to 0.1 mol kg^{-1} using hydrochloric acid 1 mol kg^{-1} .

In the feed solution, remaining hydroxide ions concentration after the use of excess sodium hydroxide to precipitate divalent metals was about 0.04 mol kg^{-1} . This value is too high for the use of the membrane and despite of accelerating the lithium transport in the first transport cycle, the selectivity is deteriorated. A good compromise between selectivity and efficiency was achieved at an initial hydroxide concentration in the feed phase of 0.02 mol kg^{-1} . Excess hydroxide ions were neutralized using hydrochloric acid 0.1 mol kg^{-1} . Transport profiles for lithium, sodium and potassium in the concentration studies involving natural seawater are shown in Fig. 10.

Lithium concentration in strip phase reaches 1.73 times the initial lithium concentration in feed phase after four cycles. The system selectivity towards sodium and specially, potassium, gets lower after each cycle. The membrane physical aging is evidenced in the membrane performance parameters deterioration. Membrane aging is faster in seawater matrix compares to that of the system in model solutions due to the high concentration of monovalent cations susceptible of being transported. Membrane degradation could be quantified by measuring the amount of LIX-54-100 lixiviated to feed solution using some spectrometric technique. However, membrane performance parameters deterioration are enough to determine if a membrane is not useful anymore. Final separation factors are 4.9 and 3.4 for sodium and potassium, respectively.

The flow diagram of the lithium extraction process from seawater is shown in Fig. 11. The final strip solution enriched with lithium is still too diluted to make proper use of it to get high purity level lithium compounds. Further solution concentration must be carried before lithium compounds precipitation [50]. Solar evaporation has been the way to go at industrial scale for lithium liquor enrichment [51] although vacuum evaporation has also been applied at pilot scale [50]. The forward osmosis using CTA based membranes has been reported for the enrichment of lithium liquors [52]. The suitability of the obtained strip solution to be used under some enrichment technique to get a high purity level compound is being further studied.

The proposed two stages precipitation process used to remove magnesium and calcium from seawater was simple and effective. The precipitate is stable and has good separability properties. However, the involved sodium hydroxide amount needed is big compared to that of the lithium content of the matrix. As a consequence of this issue, sodium concentration is risen making more complex the matrix. The magnesium and calcium precipitation protocol must be carefully studied if the lithium recovery process here proposed is going to be scaled up. An attractive alternative was recently reported by Diaz et al. who proposed membrane electrolysis to precipitate magnesium and calcium as the corresponding hydroxides [53]. The authors proposed the use of an anion exchange membrane which allows the two divalent cations hydroxides to be obtained as commercial valuable by-products without significant lithium losses [53]. The assessment of the suitability of this divalent cation removal process integration to the PIM seawater lithium extraction method is being evaluated and may be included in future work.

4. Conclusions

In this study, we firstly report the use of a PIM to selectively extract and concentrate lithium ions from alkaline diluted aqueous solutions. Extraction process finished after 6 h, time after which no appreciable lithium is transported. Undesired species like sodium and potassium are efficiently excluded in the transport process but a small fraction is transported to the strip solution. The system does not efficiently exclude divalent cations but them may be easily removed by simple precipitation procedures that do not represent an additional energy expenditure

since many lithium extraction processes currently employed already need divalent cations pre-removal.

Permeability coefficient for lithium under the optimized conditions is $2.1 \times 10^{-5} \text{ m s}^{-1}$. Selectivity of system after divalent cations removal is $\text{Li}^+ \gg \text{Na}^+ > \text{K}$. Maximal separation factors against sodium and potassium on the natural seawater matrix are 40 and 110, respectively.

The PIM was used to successfully extract and concentrate lithium from natural seawater samples. It is necessary to monitor hydronium and hydroxide concentrations in strip and feed phases, respectively, at least at the beginning of the process. Sodium and potassium selectivity is deteriorated after few extraction cycles alongside other membrane performance parameters.

The proposed protocol could be adapted to a bigger scale of continuous operation but the environmental impact of lithium removal from the marine ecosystem must be evaluated. Nonetheless, due to the immense seawater volume on earth, a global average change of just $1 \mu\text{g L}^{-1}$ would require the lithium extraction of about 1.35 million tons which is bigger than the total lithium consumption in human history [8,54].

The driving force for lithium permeation is a difference in hydronium ion concentration between feed and strip solutions. It was determined that lithium facilitated transport does not occur when feed solution has no significant hydroxide concentration. Acidic carriers like LIX-54-100 need a pH above their pKa to dissociate and form the chelate with interest species. The LIX-54-100 pKa value was not determined but it would probably lie close to that of the benzoylacetone (9.61 [55]). However, acidic carriers trend to lixiviate from the membrane if in contact with a strong alkaline media [49]. Then, a relatively narrow range must be considered for feed solution alkalinity. On the other hand, a low acid concentration is enough to provide the hydrogen ions counter transport needed to drive lithium extraction. As shown in the Vertex 10 experiments, further increasing base and acid concentrations in feed and strip solution does not further increase transport speed. A deeper study involving the membrane transport parameters as a function of driving force is needed to improve system understanding.

CRediT authorship contribution statement

Cristhian Paredes:Software, Investigation, Visualization, Writing - original draft.**Eduardo Rodríguez de San Miguel:**Conceptualization, Investigation, Supervision, Writing - review & editing.

Declaration of competing interest

The authors declare that they have no known competing financial interests or personal relationships that could have appeared to influence the work reported in this paper.

Acknowledgments

The authors would like to thank Q.F.B. María Guadalupe Espejel Maya for technical services. C. Paredes gratefully acknowledges the scholarship from the Mexican National Council for Science and Technology (CONACYT). This work was supported by DGAPA, UNAM (PAPIIT IN229219). Thanks are also due to Dra. Josefina de Gyves y Marciniak for helpful advisement during the development of the investigation and Q. Nadia Munguía Acevedo for laboratory support.

References

- [1] E.C. Evarts, Lithium batteries: to the limits of lithium, *Nature* 526 (7575) (2015) S93–S95, <https://doi.org/10.1038/526S93a>.
- [2] K. Evans, Lithium, John Wiley & Sons Ltd, 2013, pp. 230–260, <https://doi.org/10.1002/9781118755341.ch10> Ch. 10.

- [3] G. Martin, L. Rentsch, M. Höck, M. Bertau, Lithium market research – global supply, future demand and price development, *Energy Storage Mater.* 6 (2017) 171–179, <https://doi.org/10.1016/j.ensm.2016.11.004>.
- [4] J. Sterba, A. Krzemiński, P.R. Fernández, C.E. García-Miranda, G.F. Valverde, Lithium mining: accelerating the transition to sustainable energy, *Resour. Policy* 62 (2019) 416–426, <https://doi.org/10.1016/j.resourpol.2019.05.002>.
- [5] J. Speirs, M. Contestabile, The Future of Lithium Availability for Electric Vehicle Batteries, Springer International Publishing, Cham, 2018, pp. 35–57, https://doi.org/10.1007/978-3-319-69950-9_2 Ch. 2.
- [6] N. Kress, Chapter 1 - introduction, in: N. Kress (Ed.), *Marine Impacts of Seawater Desalination*, Elsevier, 2019, pp. 1–10, <https://doi.org/10.1016/B978-0-12-811953-2.00001-3>.
- [7] T. Hoshino, Preliminary studies of lithium recovery technology from seawater by electrodialysis using ionic liquid membrane, *Desalination* 317 (2013) 11–16, <https://doi.org/10.1016/j.desal.2013.02.014>.
- [8] S. Yang, F. Zhang, H. Ding, P. He, H. Zhou, Lithium metal extraction from seawater, *Joule* 2 (9) (2018) 1648–1651, <https://doi.org/10.1016/j.joule.2018.07.006>.
- [9] Y. Pranolo, Z. Zhu, C.Y. Cheng, Hydrometallurgy separation of lithium from sodium in chloride solutions using SSX systems with LIX 54 and Cyanex 923, *Hydrometallurgy* 154 (2015) 33–39, <https://doi.org/10.1016/j.hydromet.2015.01.009>.
- [10] Kunugita, Kim, Komasa, Extraction and separation of lithium and sodium by a mixed extractant of β -diketone and neutral organic phosphoric acid, *Chemical Engineering paper* 15 (3) (1989) 504–510, <https://doi.org/10.1252/kakoronbunshu.15.504>.
- [11] B. Swain, Separation and purification of lithium by solvent extraction and supported liquid membrane, analysis of their mechanism: a review, *J. Chem. Technol. Biotechnol.* 91 (2016) 2549–2562, <https://doi.org/10.1002/jctb.4976> (April).
- [12] M.S. Palagonia, D. Brogioli, F.L. Mantia, Lithium recovery from diluted brine by means of electrochemical ion exchange in a flow-through-electrodes cell, *Desalination* 475 (2020) 114192, <https://doi.org/10.1016/j.desal.2019.114192>.
- [13] F. Arroyo, J. Morillo, J. Usero, D. Rosado, H.E. Bakouri, Lithium recovery from desalination brines using specific ion-exchange resins, *Desalination* 468 (2019) 114073, <https://doi.org/10.1016/j.desal.2019.114073>.
- [14] T. Ryu, J. Shin, S.M. Ghoreishian, K.-S. Chung, Y.S. Huh, Recovery of lithium in seawater using a titanium intercalated lithium manganese oxide composite, *Hydrometallurgy* 184 (2019) 22–28, <https://doi.org/10.1016/j.hydromet.2018.12.012>.
- [15] X. Liu, X. Chen, L. He, Z. Zhao, Study on extraction of lithium from salt lake brine by membrane electrodialysis, *Desalination* 376 (2015) 35–40, <https://doi.org/10.1016/j.desal.2015.08.013>.
- [16] Y. Li, Y. Zhao, H. Wang, M. Wang, The application of nanofiltration membrane for recovering lithium from salt lake brine, *Desalination* 468 (2019) 114081, <https://doi.org/10.1016/j.desal.2019.114081>.
- [17] A. Somrani, A. Hamzaoui, M. Pontie, Study on lithium separation from salt lake brines by nanofiltration (nf) and low pressure reverse osmosis (lpro), *Desalination* 317 (2013) 184–192, <https://doi.org/10.1016/j.desal.2013.03.009>.
- [18] G. Zante, M. Boltoeva, A. Masmoudi, R. Barillon, D. Trébouet, Lithium extraction from complex aqueous solutions using supported ionic liquid membranes, *J. Membr. Sci.* 580 (2019) 62–76, <https://doi.org/10.1016/j.memsci.2019.03.013>.
- [19] T. Kinugasa, Y. Ono, Y. Kawamura, K. Watanabe, H. Takeuchi, Extraction of lithium ion from alkaline aqueous media by a liquid surfactant membrane, *J. Chem. Eng. Jpn* 28 (6) (1995) 673–678, <https://doi.org/10.1252/jcej.28.673>.
- [20] P. Ma, X.D. Chen, M. MD, Separation science and technology lithium extraction from a multicomponent mixture using supported liquid membranes, *Sep. Sci. Technol.* 35 (15) (2000) 2513–2533, <https://doi.org/10.1081/SS-100102353>.
- [21] A.D. Sharma, N.D. Patil, A.W. Patwardhan, R.K. Moorthy, P.K. Ghosh, A.D. Sharma, N.D. Patil, A.W. Patwardhan, R.K. Moorthy, Synergistic interplay between D2EHPA and TBP towards the extraction of lithium using hollow fiber supported liquid membrane, *Sep. Sci. Technol.* 51 (13) (2016) 2242–2254, <https://doi.org/10.1080/01496395.2016.1202280>.
- [22] C. Cai, F. Yang, Z. Zhao, Q. Liao, R. Bai, W. Guo, P. Chen, Y. Zhang, H. Zhang, Promising transport and high-selective separation of Li(I) from Na(I) and K(I) by a functional polymer inclusion membrane (PIM) system, *J. Membr. Sci.* 579, <https://doi.org/10.1016/j.memsci.2019.02.046>.
- [23] T. Kinugasa, H. Nishibara, Y. Murao, Y. Kawamura, K. Watanabe, H. Takeuchi, Equilibrium and kinetics of lithium extraction by a mixture of lix54 and topo, *J. Chem. Eng. Jpn.* 27 (6) (1994) 815–818, <https://doi.org/10.1252/jcej.27.815>.
- [24] G.R. Harvianto, S.-H. Kim, C.-S. Ju, Solvent extraction and stripping of lithium ion from aqueous solution and its application to seawater, *Rare Metals* 35 (12) (2016) 948–953, <https://doi.org/10.1007/s12598-015-0453-1>.
- [25] L.D. Nghiem, P. Mornane, I.D. Potter, J.M. Perera, R.W. Catrall, S.D. Kolev, Extraction and transport of metal ions and small organic compounds using polymer inclusion membranes (pims), *J. Membr. Sci.* 281 (1) (2006) 7–41, <https://doi.org/10.1016/j.memsci.2006.03.035>.
- [26] J. de Gyves, E. Rodríguez de San Miguel, Metal ion separations by supported liquid membranes, *Ind. Eng. Chem. Res.* 38 (6) (1999) 2182–2202, <https://doi.org/10.1021/ie980374p>.
- [27] M.I.G. Almeida, R.W. Catrall, S.D. Kolev, Recent trends in extraction and transport of metal ions using polymer inclusion membranes (pims), *J. Membr. Sci.* 415–416 (2012) 9–23, <https://doi.org/10.1016/j.memsci.2012.06.006>.
- [28] W. Mickler, E. Uhlemann, R. Herzschrub, B. Wenclawiak, L. Plaggenborg, The characterization of the active components in commercial β -diketone-type extractants lix 54 and mx 80 a, *Sep. Sci. Technol.* 27 (8–9) (1992) 1171–1179, <https://doi.org/10.1080/01496399208019031>.
- [29] E. Dziwinski, J. Szymanowski, Composition of cyanex® 923, cyanex® 925, cyanex®

- 921 and topo, Solvent Extr. Ion Exc. 16 (6) (1998) 1515–1525, <https://doi.org/10.1080/07366299808934592>.
- [30] S.L. Ellison, M. Thompson, Standard additions: myth and reality, Analyst 133 (8) (2008) 992–997, <https://doi.org/10.1039/b717660k>.
- [31] G. Salazar-alvarez, A.N. Bautista-flores, E. Rodríguez de San Miguel, M. Muhammed, J. de Gyves, Transport characterisation of a PIM system used for the extraction of Pb (II) using D2EHPA as carrier, J. Membr. Sci. 250 (2005) 247–257, <https://doi.org/10.1016/j.memsci.2004.09.048>.
- [32] H. Matsuoka, M. Aizawa, S. Suzuki, Uphill transport of uranium across a liquid membrane, J. Membr. Sci. 7 (1) (1980) 11–19, [https://doi.org/10.1016/S0376-7388\(00\)83181-6](https://doi.org/10.1016/S0376-7388(00)83181-6).
- [33] C.-V.I. Gherasim, G. Bourceanu, R.-I. Olariu, C. Arsene, Removal of lead(ii) from aqueous solutions by a polyvinyl-chloride inclusion membrane without added plasticizer, J. Membr. Sci. 377 (1) (2011) 167–174, <https://doi.org/10.1016/j.memsci.2011.04.042>.
- [34] D. Brown, Tracker Video Analysis and Modeling Tool, (July 2019).
- [35] F. Sun, D. Lu, J.S. Ho, T.H. Chong, Y. Zhou, Mitigation of membrane fouling in a seawater-driven forward osmosis system for waste activated sludge thickening, J. Clean. Prod. 241 (2019) 118373, <https://doi.org/10.1016/j.jclepro.2019.118373>.
- [36] A. Dickson, C. Goyet, Handbook of Methods for the Analysis of the Various Parameters of the Carbon Dioxide System in Seawater, Global Survey of Carbon Dioxide in the Oceans, U.S. Department of energy, 1994.
- [37] R Core Team, R: A Language and Environment for Statistical Computing, R Foundation for Statistical Computing, Vienna, Austria, 2019 URL <https://www.R-project.org/>.
- [38] C. Paredes, E.R. de San-Miguel, Transmem: treatment of membrane-transport data, r package version 0.1.0, URL, 2020. <https://CRAN.R-project.org/package=transmem>.
- [39] K.A. Johnson, R.S. Goody, The original Michaelis constant: translation of the 1913 Michaelis-Menten paper, Biochemistry 50 (39) (2011) 8264–8269, <https://doi.org/10.1021/bi201284u>.
- [40] C. Ritz, J.C. Streibig, Nonlinear Regression with R, Use R!, Springer-Verlag, New York, 2008, <https://doi.org/10.1007/978-0-387-09616-2>.
- [41] E. Rodríguez de San Miguel, X. Vital, J. de Gyves, Cr(vi) transport via a supported ionic liquid membrane containing cyphos il101 as carrier: system analysis and optimization through experimental design strategies, J. Hazard. Mater. 273 (2014) 253–262, <https://doi.org/10.1016/j.jhazmat.2014.03.052>.
- [42] Q.B. Chen, Z.Y. Ji, J. Liu, Y.Y. Zhao, S.Z. Wang, J.S. Yuan, Development of recovering lithium from brines by selective-electrodialysis: effect of coexisting cations on the migration of lithium, J. Membr. Sci. 548 (2018) 408–420, <https://doi.org/10.1016/j.memsci.2017.11.040>.
- [43] J. Koros, H. Ma, T. Shimidzu, Terminology for membranes and membrane processes (iupac recommendations 1996), Pure Appl. Chem. 68 (7) (1996) 1479–1489, <https://doi.org/10.1351/pac199668071479>.
- [44] W. Spendley, G.R. Hext, F.R. Himsworth, Sequential application of simplex designs in optimisation and evolutionary operation, Technometrics 4 (4) (1962) 441–461, <https://doi.org/10.1080/00401706.1962.10490033>.
- [45] J.A. Nelder, R. Mead, A simplex method for function minimization, Comput. J. 7 (4) (1965) 308–313, <https://doi.org/10.1093/comjnl/7.4.308>.
- [46] F. Walters, Sequential Simplex Optimization: A Technique for Improving Quality and Productivity in Research, Development, and Manufacturing, Chemometrics Series, CRC Press, 1991.
- [47] C. Paredes, J. Ágreda, labsimplex: simplex optimization algorithms for laboratory applications, r package version 0.1.2, URL, 2018. <https://github.com/CRparedes/labsimplex>.
- [48] G. Liu, Z. Zhao, L. He, Highly selective lithium recovery from high mg/li ratio brines, Desalination 474 (2020) 114185, <https://doi.org/10.1016/j.desal.2019.114185>.
- [49] M. Sugiura, M. Kikkawa, S. Urita, Carrier-mediated transport of rare earth ions through cellulose triacetate membranes, J. Membr. Sci. 42 (1989) 47–55, [https://doi.org/10.1016/S0376-7388\(00\)82364-9](https://doi.org/10.1016/S0376-7388(00)82364-9).
- [50] S. Nishihama, K. Onishi, K. Yoshizuka, Selective recovery process of lithium from seawater using integrated ion exchange methods, Solvent Extr. Ion Exc. 29 (3) (2011) 421–431, <https://doi.org/10.1080/07366299.2011.573435>.
- [51] B. Swain, Recovery and recycling of lithium: a review, Sep. Purif. Technol. 172 (2017) 388–403, <https://doi.org/10.1016/j.seppur.2016.08.031>.
- [52] J. Li, M. Wang, Y. Zhao, H. Yang, Y. Zhong, Enrichment of lithium from salt lake brine by forward osmosis, R. Soc. Open Sci. 5 (10) (2018) 180965, <https://doi.org/10.1098/rsos.180965>.
- [53] C.H. Díaz, N.A. Palacios, K. Verbeeck, A. PrévotEAU, K. Rabaey, V. Flexer, Membrane electrolysis for the removal of mg2+ and ca2+ from lithium rich brines, Water Res. 154 (2019) 117–124, <https://doi.org/10.1016/j.watres.2019.01.050>.
- [54] United States Geological Survey, Mineral Commodity Summaries 2019, United States Geological Survey, 2019, pp. 0–200, <https://doi.org/10.3133/70202434>.
- [55] K. Witt, E. Radzimska-Lenarcik, Studies of the aromatic β -diketones as extractant of copper ions, E3S Web of Conference, 18 2017, p. 1016, <https://doi.org/10.1051/e3sconf/20171801016>.